Multipoint Focusing of Single Ultrafast Laser Pulses

Cyril MAUCLAIR[*1], Alexandre MERMILLOD-BLONDIN[*2], Arkadi ROSENFELD[*2], Ingolf V. HERTEL[*2], Eric AUDOUARD[*1], Isamu MIYAMOTO[*3], and Razvan STOIAN[*1]

[*1] *Laboratoire Hubert Curien (UMR 5516 CNRS), Université de Lyon, Université de Saint-Etienne, 42000 Saint Etienne, France*
E-mail: razvan.stoian@univ-st-etienne.fr
[*2] *Max-Born Institut für Nichtlineare Optik und Kurzzeitspektroskopie, 12489 Berlin, Germany*
[*3] *Osaka University, Osaka 565-0871, Japan*

Designed laser foci increase the versatility of ultrafast laser pulses for 3D processing of optical materials. Typically beam engineering is employed to control the geometry of interaction and the processing dimension. Parallel photoinscription approaches were equally tested to increase the process efficiency, using a higher number of simultaneous machining points. We present here a particular photoinscription regime where a one-dimensional axial array of regular dots is generated before the region of main laser focus under single pulse exposure in fused silica and borosilicate crown glass without phase engineering. Although the interaction takes place with powers above the self-focusing level, the specific topology of the dots does not rely on nonlinear propagation but it is mainly determined by beam truncation upon focusing and subsequent diffraction. The process is explained by a linear Fresnel propagation formalism taking into account beam apodization and wavefront distortions at the air/glass interface. The array matrix can be controlled by the truncation factor and the focusing length. This photoinscription regime is employed to generate two-dimensional arrays of dots in fused silica. We show that an additional phase modulation renders flexible the pattern geometry. In addition we indicate that the pulse temporal envelope can efficiently control the form factor of laser generated individual dots.

DOI:10.2961/jlmn.2011.03.0013

Keywords: 3D laser processing, ultrashort laser pulses, parallel processing, multiple focusing, multipoints, voids, beam shaping, beam truncation, optical glasses

1. Introduction

Femtosecond laser technology represents today a flexible tool for micro-processing of transparent materials in three dimensions [1], rendering thus new optical functionalities for light transport and manipulation. When ultrashort laser pulses are focused inside a transparent solid, the nonlinear interaction between the strong electromagnetic field and the dielectric material allows for localized modifications of the matter structural characteristics. Typically, as a main result, the ultrafast exposure may modify several optical properties such as birefringence, transparence, and the refractive index on a micrometer scale [2], impacting on the optical performances. Particularly positive index changes are at the base of new concepts for integrated optics in three dimensions; from waveguides and analytic devices, up to embedded lasers or optical instrumentation (see [1] and references therein). The technique has now reached an indisputable maturity with the fabrication of several embedded photonic devices [1]. There is a strong interest in further improving the processing speed of the technique, and, in general, the structuring efficiency by multiplying the number of machining foci. With the help of wavefront tailoring devices such as spatial light modulators or diffractive optical elements involving phase engineering approaches, several groups have shown the possibility to increase the number of machined points for surface and bulk patterning [3,4] and bulk parallel writing of waveguides [5-8], alongside corrective approaches for beam propagation [8-10]. A particular domain of interest requires the formation of high contrast refractive index changes for data storage applications, where a typical solution consists of fabricating negative index changes (voids) with a contrast as high as $\Delta n=0.5$ [11-15]. This phenomenon typically arises from specific thermodynamic scenarios at high excitation levels leading to material thermo-mechanical expansion, shock generation with rarefaction, and, eventually, gas-phase transitions. Typical examples of voids induced in conditions of tight and moderate focusing of a single fs laser pulse in the bulk of a borosilicate glass and fused silica are given in Figure 1(a,b).

As yet another solution to multipoint machining, the self-formation of regular voids under the accumulation of many light pulses was reported, where the spacing, size and number of voids depend on the accumulation dose and the pulses energy [16-18]. This method is particularly powerful as it does not require external beam engineering devices, relying instead on the material response and its transient effect on the characteristics of laser matter interaction. As to its origin, several hypotheses have been put forward. The main aspects include: (a) nonlinear propagation as a succession of self-focusing and defocusing axial zones due to Kerr nonlinearity and the emerging carrier plasmas [19], ensuring multiple refocusing points, (b) axial intensity modulation due to spherical aberration at the air-dielectric

interface [16,20], or (c) nucleation of voids in a low viscosity glass phase [21,22]. Typically the former processes can be induced by single pulses, while the latter requires a certain degree of incubation, i.e. accumulation of consecutive pulses. Overall, this implies that, in spite of the fact that rather tightly focused femtosecond pulses confine severely the energy in the focal region [23], in particular conditions the modified area can extend after the focus, yielding consecutive voids with quite regular spacing [17,18]. This represents a natural solution for achieving regular void arrays. Typical examples of void generation in the above-mentioned conditions are given in Fig. 1(b-d), emphasizing in moderate focusing conditions the role of nonlinear propagation, spherical aberration effects on propagation, and incubation effects.

The topic of this work aligns with the efforts of developing single shot multipoint techniques without the assistance of spatial beam modulators. Employing ultrashort laser pulses, we present a novel photoinscription regime [24] allowing for single step multispot bulk writing without extrinsic user-induced wavefront manipulation and occurring with a single laser pulse. This determines the generation of regular micrometric modifications on the axis before the region of main focus with examples given here in fused silica (FS) and borosilicate crown glass (BK7). The photowriting regime we emphasize here has the significant advantage that only one light pulse suffices to generate tens of permanent dots without the need of spatial beam shaping systems.

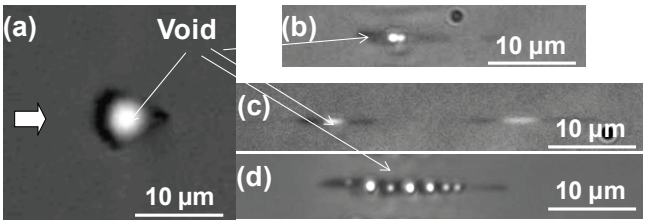

Fig. 1 (a) Single shot induced void in D263 borosilicate glass under tight focusing conditions (NA=1.25, 1.5 µJ/pulse, 160 fs). (b) Single shot void formation in FS under moderate focusing (NA=0.45, 0.5 µJ/pulse, 160 fs). (c) Single shot multi void formation in FS under moderate focusing (NA=0.45, 0.5 µJ/pulse, 160 fs) in the presence of spherical aberrations (focusing depth 1mm). (d) The onset of multiple voids in FS using multipulse irradiation above the critical power for self-focusing (NA=0.45, 1 µJ/pulse, 160 fs, N=50). The laser pulse is incident from the left.

2. Experiment

Typically FS and BK7 samples were irradiated with 160 fs pulses from an 800 nm Ti:Sapphire amplified ultrafast laser system operating at 160 Hz. Single pulses selected with a synchronized electromechanical shutter were focused inside the target by a microscope objective with a nominal numerical aperture (NA) of 0.45, in the vicinity of the surface in order to reduce wavefront distortions. In particular cases mentioned in the text higher numerical apertures were used (NA=1.25) as well as a second type of borosilicate glass (D263). The relative ratio between the beam diameter and the objective pupil determines different truncation factors T and slightly smaller effective numerical apertures for T<2. The laser-induced structures were observed with a Zernike-type positive optical phase-contrast microscopy (PCM) system coupled to a high-resolution CCD camera providing a side-image of the relative changes in the refractive index induced by the irradiation. Positive and negative refractive index changes correspond to the image dark and white areas, respectively, the voids being identifiable via the intense white color. Equally, dynamic optical transmission microscopy (OTM) was performed, where, replacing the standard illumination with a fs laser pulse time-correlated with the excitation pulse allows for a time-resolved introspection [25] into the transient optical modifications.

3. Discussion

Fig. 1 shows bulk modifications in FS, subsequent to single femtosecond pulse irradiation for various pulse energies. The laser focus is situated 200 µm beneath the material's surface, in conditions of negligible spherical aberrations [26]. This location corresponds to the structures generated with the lowest pulse energy at the bottom of Fig. 2. As indicated in the figure, the interaction topology can be divided in several interaction regimes. If low pulse energies are usually leading to interaction levels corresponding to positive index and therefore waveguide formation, the high energy region indicates the formation of a series of dot arrays arranging before the main focus and extending to the laser source with increasing energy.

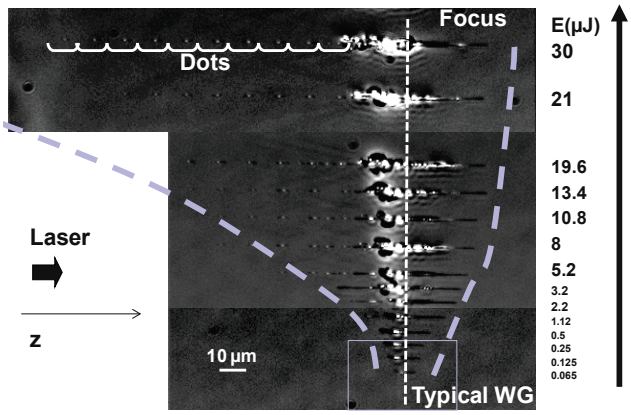

Fig. 2 PCM pictures of single pulse irradiation effects in FS at different pulse energies (E). The laser propagates along the z-axis from the left (NA=0.45). For sufficient pulse energy (above 5 µJ), a particular photowriting regime occurs where regularly spaced dots appear up to 200 µm before the focal area upon single pulse irradiation in both glasses. Typical waveguide (WG) photoinscription regions are also indicated at low energies.

The dot array, located before the geometrical focus, shows a regular spacing, with a period of about 10 µm. A natural question concerns the reason of the regular structure formation. The gradual extension towards the laser source invites to assume the influence of nonlinear propagation. However, the fact that the dot position is independent of the energy or pulse duration leads to believe that another mechanism is at work, as detailed in the next paragraphs.

Firstly, by using the time-resolved OTM, we note that the excitation dynamics in the regions of the dots and the

focal region have the same characteristics, being induced by the same pulse at local intensity levels above the permanent modification threshold. The dot position corresponds to regions of high density electron-hole plasma in the glass samples. Fig. 3 shows the development of the electron plasma with images at the peak of excitation and during relaxation, the dots being visible by the accumulation of excited carriers (absorptive dark regions in OTM, probed at 400 nm wavelength) [25].

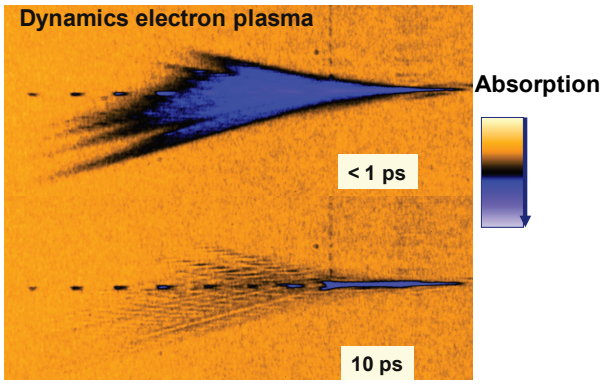

Fig. 3 OTM snapshots of the electron plasma relaxation in FS after ultrafast laser excitation (160fs, pulse from the left), probed at 400 nm observation wavelength with sub-ps duration. The energy is approximately 40 µJ. The corresponding time moments are given. They correspond to the excitation peak (top) and a relaxed phase (bottom).

We will discuss below particular features of this interaction regime in two materials. Fig. 4 shows the onset of the dot array in FS and BK7. In the moderate energetic regimes below 2 µJ, we note a drastic difference in the response of BK7 and FS under laser irradiation as already reported [23]. While the response of BK7 is dominated by thermal expansion in a large region resulting in the onset of a low density material [27] as consequence of a high expansion coefficient, the response of FS is characterized by the appearance of a reduced white zone in PCM corresponding to a void [11], and a filament of higher refractive index. As indicated above, time-resolved investigations associated the void with the region of stronger absorption of the electronic plasma and subsequent local mechanical rarefaction [25].

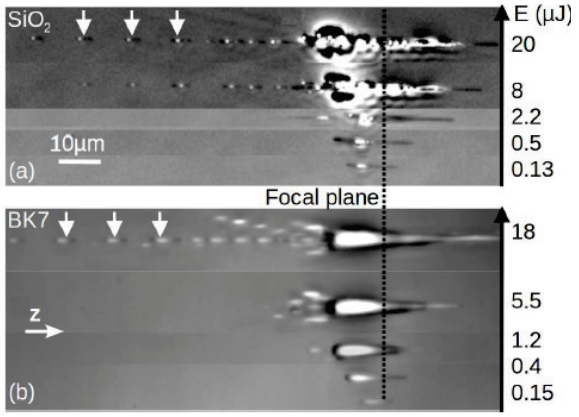

Fig. 4 Comparison of single pulse irradiation effects in FS and BK7 at different pulse energies (E). The laser propagates along z from the left (NA=0.45).

The new photoinscription regime is clearly observable on the traces obtained at the highest energies in Fig. 4 and corresponds to powers (tens of MW) severely exceeding the critical power for self-focusing in both glasses (few MW). A very regular succession of dots (see arrows) aligned on the laser propagation axis *z* precedes the area of main focusing in both glasses. We observed that this line can extend to the sample surface if sufficient pulse energy is employed. The local mapping of these pre-dots is quasi-identical in both materials which can be surprising since those glasses are known to behave very differently under femtosecond exposure [23].

In the context of femtosecond processing, it is tempting to assign the cartography of these structures to nonlinear propagation in the form of a regular succession of self-focusing and plasma defocusing phenomena, with repetitive concentration of light. In fact, it was shown that loose focusing conditions favoring filamentary propagation permit the photowriting of various modulated permanent structures [28]. However, a succession of self-focusing points strongly depends on the peak intensity and temporal characteristics of the pulse [29]. We conducted studies varying the pulse duration to validate this hypothesis (not shown). Investigations with longer pulses revealed that the position of the dots stays identical for pulse durations under 1 picosecond. For longer pulses, the dots do not appear. Also, comparing the 20 µJ and the 8 µJ irradiation traces in FS [Fig. 4 (a)] shows that the position of the dots stays identical regardless of the pulse peak intensity, thus not validating the nonlinear propagation for being responsible for the dots mapping.

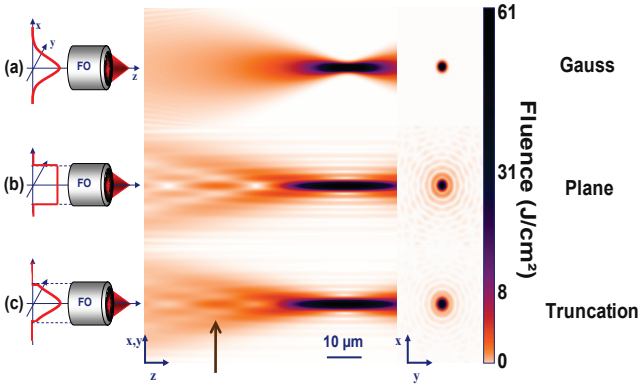

Fig. 5 Typical focusing patterns in air of a aperture-free Gaussian (a), apertured plane wave (b), and truncated Gaussian beam via an objective pupil (NA=0.25) (c), illustrating the onset of fluence peaks before the focus as an effect of truncation. The corresponding axial and the transverse fluence patterns are shown (center and right) for the specific intensity distributions at the lens plane (left). Calculation conditions: (a) focal f=4mm, waist *w*=1mm, (b) pupil radius *r*=1mm, and (c) *r*=1mm and *w*=1mm. Input energy 1µJ.

Coming back to the dot distribution, interestingly, the distance separating two consecutive dots is slightly smaller in FS than in BK7, following the tendency of their respective refractive indices at 800 nm (n_{FS}=1.453 and n_{BK7}=1.509). This distance is affected by the focal length of the focusing element and by the limiting factor of the objective with respect to the beam transverse dimensions.

These observations motivated us to precisely calculate the laser beam linear propagation using a Fresnel propagation code [24,30] in order to determine the irradiation pattern over the focal volume.

The linear focusing characteristics of an idealized beam with Gauss distribution, plane wave, or truncated wavefronts in air are represented in Fig. 5. The non-truncated Gaussian propagation shows no pre-focus modulation [Fig. 5 (a)] whereas the truncation [Fig. 5 (b,c)] induces modulation of axial intensity due to the interference of diffracted wavelets, pointing thus the role of aperturing the beam. We indicate below for the optical case employed here the results of the model.

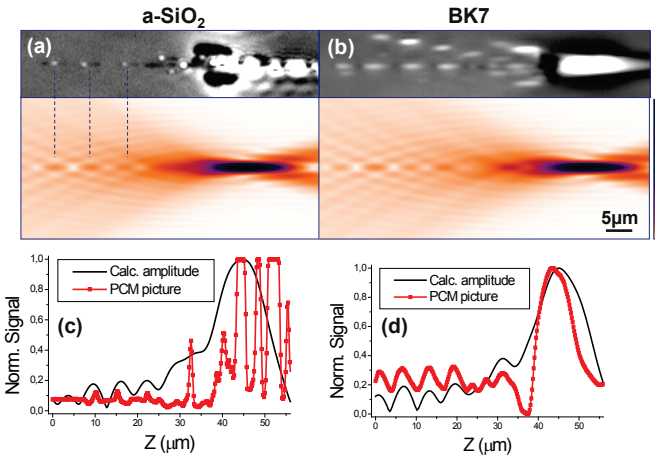

Fig. 6 (a,b) PCM pictures (top) of single pulse irradiation effects in FS and BK7 and the comparison with the Fresnel propagation results (bottom). The dashed lines show the correspondence between the position of the dots and the calculated fluence peaks. (c,d) Horizontal axial cross-section of the PCM picture (red symbols) and of the numerical results (black line) for FS and BK7.

Within the paraxial approximation and neglecting spectral effects, the transverse intensity profile $I(x', y')$ of a complex laser field $\tilde{A}(x, y)$ focused by a lens of focal length f after the propagation over the distance D is given by:

$$I(x',y') \propto \left| F_{f_{x'}f_{y'}} \left[\tilde{A}(x,y) e^{-\frac{i\pi}{\lambda}\left(x^2+y^2\right)\left(\frac{1}{D}-\frac{1}{f}\right)} \right] \right|^2$$

where $F_{fx'fy'}$ is the two-dimensional (2D) Fourier Transform with respect to the spatial frequencies in the (x', y') plane. For a non-truncated collimated Gaussian beam, $\tilde{A}(x, y)$ reduces to a Gaussian function and the calculated fluence around the focus shows a single fluence peak at the beam waist [see Fig. 5 (a)]. The focus landscape for a truncated planewave is given in Fig. 5(b). An axial modulation of intensity becomes visible, with a corresponding cross-sectional Airy pattern. For a truncated Gaussian, the effect of beam truncation from the focusing lens aperture can be incorporated in $\tilde{A}(x, y)$ with a rect function, resulting in a modulated fluence map showing the appearance of fluence peaks before the main focus as illustrated in Fig. 5 (c). The truncation factor T is the ratio between the Gaussian beam diameter at the $1/e^2$ intensity point and the lens aperture diameter and is close to unity in our experiments and calculations. We first calculated the phase and amplitude of the laser beam after propagation from the lens until the air/glass interface. Then a phase term was added to the laser spatial phase to take into account the phase distortion due to the refraction. The analytical expression of this additional phase term $\psi(\rho)$ is easily obtained from geometrical considerations [9] and reads $\psi(\rho) = d(n_2\cos\theta_2 - n_1\cos\theta_1)$, where n_1 and n_2 are the optical indices of air and glass respectively. The distance d separates the sample surface and the geometrical focus when $n_2=n_1$. The angle θ_1 is linked to the lens NA and to the normalized pupil radius ρ by $\rho = \sin\theta_1/NA$. The angle θ_2 is defined from the Snell-Descartes law: $n_1\sin\theta_1 = n_2\sin\theta_2$. The propagation through the air/glass interface is accompanied by a certain amount of reflection depending on the incidence angle and the beam polarization. We took into account the associated variation of amplitude using the corresponding Fresnel coefficients. The beam polarization is in the incidence plane, parallel to the microscopy images shown here.

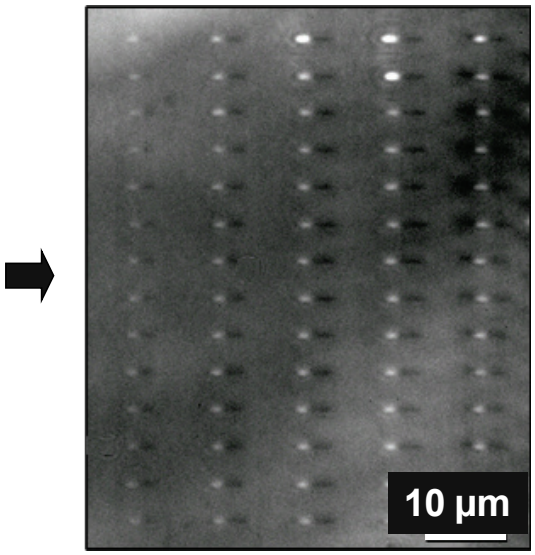

Fig. 7 Array of dots written in FS in the multidot photoinscription regime. Each line was written with a single pulse (direction indicated by the arrow). The main damage (not shown) is situated on the right.

The propagation calculations were then carried out for an ensemble of X-Y planes comprising the focal area. Fig. 6 shows the calculated focal fluence maps for FS and BK7 with the PCM pictures of the bulk modification [respectively Fig. 6(a) and (b), top and bottom parts]. The calculated fluence peaks preceding the focus precisely match the dots position (see the vertical dashed lines). A horizontal cross section along the optical axis of the PCM picture and the simulations is shown in Fig. 6 (c) and (d) for FS and BK7. The mapping of the on-axis dots is clearly verified by the Fresnel propagation results.

As an illustration of the potential applications of this photowriting regime, a 2D array of dots is presented in Fig. 7. The numerous dots shown on the figure were written with only 14 single pulse exposures, this illustrating the possibility to write many structures with a high throughput. Those modifications can be used as data points or arrays of waveguides or phase gratings (i.e with a continuous irradiation under transversal displacement of the sample).

The next step is to show that the dots position and number can be controlled to render this photowriting regime more appealing for data storage or multi-waveguide writing by higher flexibility [24]. As the multidots appear due to the interference of several wavelets with specific orientation of the wave-vectors, a phase-only spatial modulation appears as an appropriate way to achieve the dots position control while preserving a high energetic exposure. As an illustration of this potentiality induced by additional phase-engineering means, 2D phase modulations were numerically calculated with the help of an evolutionary algorithm in order to produce user-defined dots mapping. Fig. 8 shows the resulting numerical intensity profiles for three different optimized phase modulations illustrating the possibility to photowrite arbitrary binary data sequences.

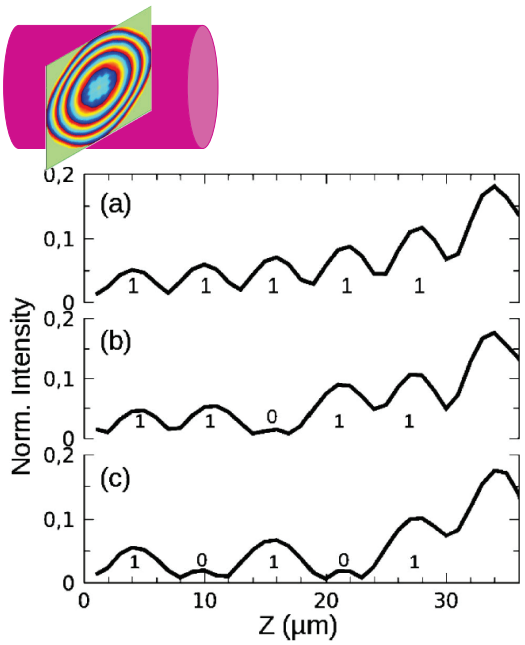

Fig. 8 Calculated intensity profiles along the optical axis z just before the main focus for different wavefront modulations controlling the dots local mapping and intensities. (a) no phase modulation yielding "11111" sequence. (b) and (c) various modulations yielding "11011" and "10101". The top part schematically illustrates the wavefront modulation.

A final issue is related to the pulse aspect form. The longitudinal size of the void can be influenced by controlling the nonlinear pulse propagation, with consequences on the energy confinement. A natural way for performing this task lies on intensity delivery that controls equally the nonlinearity of the environment and the sequence of excitation.

Using a temporal pulse tailoring method [26], the geometry of excitation can be drastically changed, as indicated in Fig. 9 for two materials and two focusing conditions. Elongated or spherical forms can be obtained depending on the focusing conditions and the pulse duration. As a function the focusing conditions, the pulse duration can affect the nonlinear propagation in two particular ways. In case of tight focusing, this occurs by reducing the excitation efficiency, and, in the case of moderate focusing, by concentrating the energy in the focal region, as, for a longer sequence, the plasma appears latter in the pulse and its defocusing effect strongly diminishes. Thus, the geometry of the voids is significantly affected by the pulse form [31].

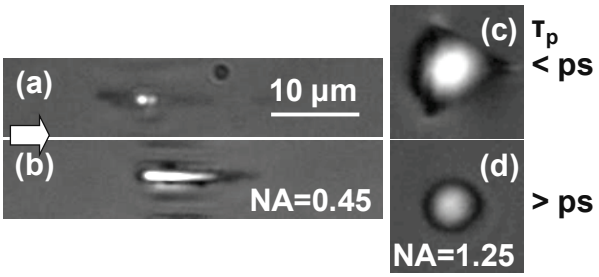

Fig. 9 Transformation of void aspect form with the pulse duration. (a,b) Moderate focusing (NA=0.45) in fused silica for 0.16 ps (a) or 4 ps (b). (c,d) Tight focusing (NA=1.25) in borosilicate D263 for 0.16 ps (c) or 10 ps (d).

4. Conclusions

In conclusion, we described here a novel single pulse photoinscription regime leading to parallel structuring, where a uni-dimensional axial array of regular dots is generated before the main laser focus area in various glasses. The dots topology matches the fluence peaks calculated from Fresnel linear propagation simulations deriving essentially from the beam truncation. As an illustration, a 2D array of dots in FS is achieved in this processing window. An additional employment of spatial phase modulation increases the flexibility of the process, leading to patterns at designed locations. The aspect form of the dots can be changed by varying the temporal characteristics of the laser pulse.

Acknowledgments

The support of the Agence Nationale de la Recherche and Saint Etienne Metropole is gratefully acknowledged

References

[1] K. Itoh, W. Watanabe, S. Nolte, and C. B. Schaffer, MRS Bull., 31, (2006) 620.
[2] E. Bricchi, B. G. Klappauf, and P. G. Kazansky, Opt. Lett., 29, (2004) 119.
[3] Y. Kuroiwa, N. Takeshima, Y. Narita, S. Tanaka, and K. Hirao, Opt. Express 12, (2004) 1908.
[4] S. Hasegawa, Y. Hayasaki, and N. Nishida, Opt. Lett., 31, (2006) 1705.
[5] C. Mauclair, G. Cheng, N. Huot, E. Audouard, A. Rosenfeld, I. V. Hertel, and R. Stoian, Opt. Express, 17, (2009) 3531.
[6] M. Pospiech, M. Emons, B. Väckenstedt, G. Palmer, and Uwe Morgner, Opt. Express, 18, (2010) 6994.
[7] M. Sakakura, T. Sawano, Y. Shimotsuma,1 K. Miura, and K. Hirao, Opt. Lett., 36 (2011) 1065.
[8] A. Jesacher and M. J. Booth, Opt. Express, 18, (2010) 21090.
[9] M. J. Booth, M. A. A., Neil, and T. Wilson, J. Micros. 192, (1998) 90.
[10] C. Mauclair, A. Mermillod-Blondin, N. Huot, A. Audouard, and R. Stoian, Opt. Express, 16, (2008) 541.

[11] E. N. Glezer and E. Mazur, Appl. Phys. Lett., 71, (1997) 882.
[12] R. Taylor, C. Hnatovsky, and E. Simova, Laser and Photon. Rev., 2, (2008) 26.
[13] S. Juodkazis, V. Mizeikis, M. Sudžius, H. Misawa, K. Kitamura, S. Takekawa, E. G. Gamaly, W. Z. Krollkowski, and A. V. Rode, Appl. Phys. A, 93, (2008) 129.
[14] Y. Hayasaki, T. Sugimoto, A. Takita, and N. Nishida, Appl. Phys. Lett., 87, (2005) 031101.
[15] M. J. Booth, M. Schwertner, T. Wilson, M. Nakano Y. Kawata, M. Nakabayashi, and S. Miyata, Appl. Phys. Lett., 88, (2006) 031109
[16] J. Song, X. Wang, X. Hu, Y. Dai, J. Qiu, Y. Cheng, and Z. Xu, Appl. Phys. Lett., 92, (2008) 092904.
[17] S. Kanehira, J. Si, J. Qiu, K. Fujita, and K. Hirao, Nano Lett., 5, (2005) 1591.
[18] E. Toratani, M. Kamata, and M. Obara, Appl. Phys. Lett., 87, (2005) 171103.
[19] A. Couairon and A. Mysyrowicz, Phys. Rep., 441, (2007) 47.
[20] C. Hnatovsky, R. S. Taylor, E. Simova, V. R. Bhardwaj, D. M. Rayner, and P. B. Corkum, J. Appl. Phys. 98, (2005) 013517.
[21] W. Watanabe, and K. Itoh, Opt. Express 10, (2002) 603.
[22] K. Mishchik, G. Cheng, G. Huo, I. M. Burakov, C. Mauclair, A. Mermillod-Blondin, A. Rosenfeld, Y. Ouerdane, A. Boukenter, O. Parriaux, and R. Stoian, Opt. Express, 18 (2010) 24809.
[23] V. R. Bhardwaj, E. Simova, P. B. Corkum, D. M. Rayner, C. Hnatovsky, R. S. Taylor, B. Schreder, M. Kluge, and J. Zimmer, J. Appl. Phys., 97, (2005) 083102.
[24] C. Mauclair, A. Mermillod-Blondin, S. Landon, N. Huot, A. Rosenfeld, I. V. Hertel, E. Audouard, I. Myiamoto, and R. Stoian, Opt. Lett., 36, (2011) 325.
[25] A. Mermillod-Blondin,J. Bonse, A. Rosenfeld,1 I. V. Hertel, Yu. P. Meshcheryakov, N. M. Bulgakova, E. Audouard, and R. Stoian, Appl. Phys. Lett., 94, (2009) 041911.
[26] N. Huot, R. Stoian, A. Mermillod-Blondin, C. Mauclair, and E. Audouard, Opt. Express, 15, (2007) 12395.
[27] A. Mermillod-Blondin, I. M. Burakov, Yu. P. Meshcheryakov, N. M. Bulgakova, E. Audouard, A. Rosenfeld, A. Husakou, I. V. Hertel, and R. Stoian, Phys. Rev. B 77, (2008) 104205.
[28] K. Yamada, W. Watanabe, Y. Li, K. Itoh, and J. Nishii, Opt. Lett., 29, (2004) 1846.
[29] G. Heck, J. Sloss, and R. J. Levis, Opt. Commun., 259, (2006) 216.
[30] N. Huot, N. Sanner, and E. Audouard, J. Opt. Soc. Am. B, 24, (2007) 2814.
[31] A. Mermillod-Blondin, C. Mauclair, A. Rosenfeld, J. Bonse, I. V. Hertel, E. Audouard, and R. Stoian, Appl. Phys. Lett., 93, (2008) 021921.

(Received: August 02, 2011, Accepted: November 21, 2011)